Available online at www.sciencedirect.com
SCIENCE DIRECT
Journal of Magnetic Resonance 180 (2006) 105–109
JMR Journal of Magnetic Resonance
www.elsevier.com/locate/jmr

Selective detection of ordered sodium signals via the central transition

Jennifer Choy, Wen Ling, Alexej Jerschow *

Chemistry Department, New York University, New York, NY 10003, USA

Received 8 November 2005; revised 19 January 2006
Available online 15 February 2006

Abstract

Given the correlation between the concentrations of ordered ^{23}Na and the onset of tissue disorders, the ability to select the signal from ordered ^{23}Na over that of free ^{23}Na is of particular importance and can greatly enhance the potential of ^{23}Na-MRI as a diagnostic tool. Here, we describe a simple method that selectively detects the central transition of ordered sodium while minimizing the signal from free sodium. Our method relies upon the influence of the quadrupolar interaction on nutation frequencies and may also benefit solid-state imaging experiments. Both a liquid crystalline environment and a cartilage sample are used to demonstrate a clean separation between anisotropic and isotropic regions in the experiments.

Keywords: Nutation; Double-quantum filter; Sodium-MRI; Ordered sodium; Quadrupolar coupling; Cartilage imaging

1. Introduction

The large abundance of ^{23}Na in living tissues, especially in areas of brain and cartilage, offers promising prospect for ^{23}Na-MRI as a powerful diagnostic method for cartilage pathologies, as well as for studying brain tumors [1]. While both free and ordered (bound) sodium are prevalent throughout the body, monitoring the levels of the latter is of particular interest due to the anticipated strong correlation between the changes in the ordered sodium concentration and the early symptoms of most cartilage disorders. For instance, proteoglycan depletion, which often accompanies the onset of bone and cartilage diseases, such as arthritis, is consistent with a decrease in ordered sodium levels [2–8]. In addition, sodium plays a direct role in regulating cell mitosis and proliferation and there is an increase of about 350% in sodium concentration in malignant tumor cells in comparison to normal cells [1]. This discrepancy renders ^{23}Na-MRI an excellent candidate for examining tumors. Frequently, the signal from free sodium overlaps with the central transition of ordered sodium, making exact measurements of the preferred signal from ordered sodium difficult. Methods that make possible the selective observation of signals arising from ordered sodium can therefore greatly enhance the potential for ^{23}Na-MRI in studying living tissues.

Techniques that have already been developed to selectively detect sodium signals from ordered environments mostly depend on the evolution properties of the magnetization components under the action of the quadrupolar coupling. For example, one can exploit the influence of the quadrupolar interaction on the evolution of the system by performing double-quantum filter experiments to detect the double-quantum coherence terms ($T^2_{\pm 2}$ in spherical tensor operator representation), which are created from transverse magnetization operators $T^1_{\pm 1}$ under the action of the quadrupolar coupling [9,10]. Multiple-quantum coherences may also be created through relaxation-induced evolution [11], which may lead to complications when a clean selection of ordered sodium is desired. Alternatively, the Jeener–Broeckaert experiment relies on the rotational properties of tensors of different rank for this selection [2]. Both the double-quantum filter and the Jeener–Broeckaert methods were later adapted to detecting the filtered signals via the central transition, thus providing higher signal-to-noise ratios, as well as, higher resolution

* Corresponding author. Fax: +1 212 260 7905.
E-mail address: alexej.jerschow@nyu.edu (A. Jerschow).

1090-7807/$ - see front matter © 2006 Elsevier Inc. All rights reserved.
doi:10.1016/j.jmr.2006.01.011

[9]. These modifications require, however, a large number of phase cycling steps to cleanly select the desired signals, and become sensitive to B_0 and B_1 inhomogeneities. A method based on the suppression of the central transition signal was developed recently (central peak suppression, CPS) [12]. Later, we described a method, which employs frequency-swept pulses for this purpose. Using this approach, frequency-selective filtering can be achieved, so that only sodium experiencing a certain range of quadrupolar couplings contributes to the detected signal [13,14].

The purpose of the present study was to provide another approach to minimizing the signal from free sodium thus allowing for the selective detection of the central transition of ordered sodium. Here, we take advantage of the fact that spin-$\frac{3}{2}$ nuclei (i.e., ordered ^{23}Na) having a non-vanishing quadrupolar interaction term in the Hamiltonian evolve differently in the presence of radiofrequency (rf) fields depending on the ratio between the nutation frequency (ω_{rf}) and the quadrupolar coupling constant (ω_Q). Free ^{23}Na, meanwhile, is located in isotropic environments and therefore is not subject to influence by the quadrupolar interaction. We demonstrate this selection using a liquid crystalline environment, as well as, a cartilage sample, where we selectively detect the central transition of the ordered ^{23}Na NMR signal from a mixture of free and ordered environments. The advantage of this method lies in its simplicity, which makes it particularly easy to be incorporated into existing imaging protocols. The experiments on a cartilage sample also show a significant robustness to B_0 inhomogeneity effects.

2. Theory

The quadrupolar interaction arises from the electrostatic interactions between nuclear and electric-charge distributions. The orientational dependence of this interaction arises as a consequence of the truncation by the Zeeman interaction [15]. In this case, the interaction can be written as

$$H_Q = \frac{A_Q}{2}\left[I_z^2 - \frac{I(I+1)}{3}\right] \tag{1}$$

with the time-averaged quadrupolar coupling constant A_Q given (in units of angular frequency) by

$$A_Q = \left\langle \left[P_2(\cos\beta) + \left(\frac{\eta}{2}\right)\cos 2\alpha \sin^2\beta\right] 3\omega_Q \right\rangle, \tag{2}$$

where

$$\omega_Q = \frac{e^2qQ}{2I(2I-1)} \tag{3}$$

and eq and eQ, respectively, represent the zz-components of the electric field gradient and the nuclear electric quadrupole moment. η denotes the anisotropy parameter and is assumed to be zero if the system is cylindrically symmetric. The Euler angles α, β, and γ relate the principal axis frame to the laboratory frame. The Hamiltonian on-resonance in the rotating frame becomes

$$H_{total} = H_Q + H_{rf}. \tag{4}$$

In the regime where $\omega_{rf} \gg A_Q$, we may neglect H_Q. A 90° pulse is obtained when $\omega_{rf}\tau_p = \frac{\pi}{2}$, where τ_p is the pulse duration. In the regime where $\omega_{rf} \ll A_Q$, the first maximum of the central transition signal appears at $\omega_{rf}\tau_p = \frac{\pi}{4}$, apparently under the action of a doubled effective rf field [16]. For higher half-integer spins one can show that the effective rf field acting selectively on the central transition is enhanced by a factor of $(I+\frac{1}{2})$. These effects form the basis of nutation spectroscopy [17].

3. Experimental

All experiments were carried out on a Bruker Avance 500 MHz spectrometer with a BBI probe tuned to sodium frequency. The spectrometer is equipped with a single-axis gradient accessory with a maximum strength of 53 G/cm.

The liquid crystalline sample was prepared by placing two capillaries (i.d. 1 mm, o.d. 1.5 mm) in an NMR tube and filling them with different solutions. One capillary contains a liquid crystal solution composed of 38.8 wt% sodium decyl sulfate (SDS), 6.7 wt% decanol, and 54.5 wt% H_2O, and the other was filled with a 1 M NaCl solution, representing sodium in ordered and free environments, respectively. The SDS solution gives rise to a quadrupolar splitting of approximately 10 kHz. The void space outside of the capillaries was filled with D_2O to obtain a lock signal. The schematic of the sample is displayed in Fig. 3A.

The cartilage sample was prepared by cutting a sample of diameter 3.2 mm and height 3 mm from a bovine cartilage sample (Bierig Bros, Vineland, NJ) and placing it at the bottom of a Shigemi NMR tube. A fluorinated oil solution (fluorinert FC77, Aldrich) was added to a level of 11 mm (top meniscus) and 3.5 mm of a 50 mM sodium solution was added at the top (measured from the top fluorinert meniscus to bottom of the water meniscus). Fluorinert FC77 is heavier than water ($\rho = 1.78$ g/ml) and remains below the water solution. The sample was not covered and the air region was deliberately placed within the active coil volume. The saline solution was prepared by dilution from a phosphate-buffered saline stock solution (Aldrich, pH 7.4, 138 mM NaCl). A schematic of this sample is shown in Fig. 4B.

The pulse sequence used is shown in Fig. 1, which consists of a soft $\frac{\pi}{2}$ pulse (the pulse angle refers to the effect on free sodium), followed by a hard $\frac{\pi}{2}$ pulse for detection. For abbreviation, we will address this sequence as quadrupolar filter by nutation (QFN) for the rest of this article. We varied the rf strength of the first (selective) pulse to examine the sensitivity of this method to changes in $\frac{\omega_{rf}}{A_Q}$. All pulse durations were calibrated based on the free sodium signal. The rf strengths were $\frac{\omega_{rf}}{2\pi} = 20.4$ kHz for the hard pulses (12 μs 90° pulse duration) and $\frac{\omega_{rf}}{2\pi} = 556$ Hz for the soft pulse in the liquid crystalline sample (450 μs pulse duration), and $\frac{\omega_{rf}}{2\pi} = 50$ Hz for the cartilage sample (5 ms pulse

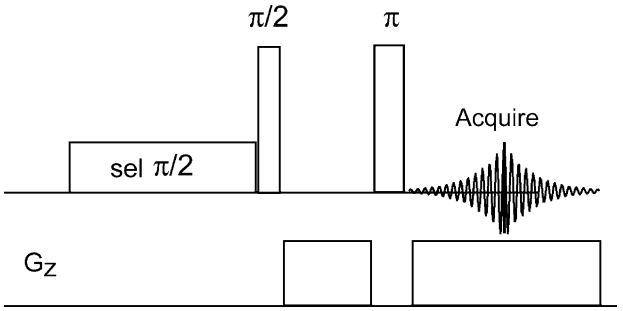

Fig. 1. Pulse sequence of the quadrupolar filter by nutation (QFN) experiment performed in combination with a gradient spin echo.

duration). The CPS experiment (Fig. 4A) was performed using a 15 ms soft pulse with 10 Hz power, and a hard pulse of 2 μs duration and 20.4 kHz power.

The 1D imaging profiles were obtained using a gradient spin echo sequence, as represented in Fig. 1, with an echo time of 2 ms. The gradient strength was 4.2 G/cm for the liquid crystalline sample and 2.1 G/cm for the cartilage sample. Two thousand and forty-eight data points were acquired to cover a spectral window of 50 kHz, with 64 (liquid crystal) and 32 (cartilage) transients coadded. The pulses were executed with a four-step phase cycle, in which ϕ_1, the phase of the first pulse, was stepped through the values of 0°, 90°, 180°, and 270°, and the receiver phase was left constant. The repetition delay was 500 ms for both samples.

The relaxation parameters of the two samples were measured using an inversion recovery and a CPMG method. Only one component was fit to the decay. For the liquid crystalline sample $T_1 = 14$ ms, $T_2 = 10$ ms, for the cartilage sample $T_1 = 13.4$ ms, $T_2 = 8.3$ ms, and for the saline solution $T_1 = 47.4$ ms, $T_2 = 47$ ms.

Simulations were performed using MATLAB [18] to gain insight into the evolution of the quadrupolar spin-$\frac{3}{2}$ nuclei under rf excitations with varying strengths, and, specifically, to study how the central transition intensity of the ordered sodium signal changes with $\frac{\omega_{rf}}{A_Q}$ during the QFN sequence.

4. Results and discussion

The QFN pulse sequence, as represented in Fig. 1, exploits the rotational properties of the quadrupolar spin system, thus making possible the preferential selection of the signal from the ordered sodium central transition over that from free sodium. The spins in both the free and ordered environments are initially aligned along the z-magnetization direction. The first selective $\frac{\pi}{2}$ pulse has the effect of aligning the magnetization of the free sodium spin along the transverse direction while inverting the central transition populations of the ordered sodium spin. The hard readout pulse puts the free sodium spin back along z and puts the central transition from the ordered sodium into the transverse plane, where it can be detected.

Our pulse calibrations were subject to constraints from instrumentation, as well as those set forth by relaxation considerations. As noted previously, the nutation frequencies are $\frac{\omega_{rf}}{2\pi} = 20.4$ kHz for the hard pulse and $\frac{\omega_{rf}}{2\pi} = 556$ Hz for the soft pulse, which, considering a quadrupolar coupling constant of about 10 kHz for ^{23}Na in the liquid crystal, yield ratios of $\frac{\omega_{rf}}{A_Q}$ of around 2 and 0.056. For the cartilage sample, assuming a residual quadrupolar coupling constant centered at approximately 375 Hz (derived from the satellite transition splitting in Fig. 4) the ratios are 54.4 and 0.13, respectively. Although these values are perhaps not deemed to be ideally representative of the $\frac{\omega_{rf}}{A_Q} \ll 1$ and $\frac{\omega_{rf}}{A_Q} \gg 1$ regimes, our simulations show how robust the pulses are in approximating these cases.

In Fig. 2, we show simulations of the full QFN sequence to better elucidate the behavior of the spin-$\frac{3}{2}$ quadrupolar system in regimes with different ratios of $\frac{\omega_{rf}}{A_Q}$ for the first $\frac{\pi}{2}$ pulse, and the hard pulse power of 20.4 kHz. Here, we plot the central transition intensity against $\frac{\omega_{rf}}{A_Q}$, for $0.01 \leqslant \frac{\omega_{rf}}{A_Q} \leqslant 2$, a range that is well within our experimental confines. For $\frac{\omega_{rf}}{A_Q}$ greater than approximately 0.3, the curve drops with increasing $\frac{\omega_{rf}}{A_Q}$. These simulations show that the soft pulse ratios used in our experiments are sufficiently small to achieve the very efficient selective excitation performed in the QFN experiment.

The 1D images obtained in the liquid crystalline experiments are displayed in Fig. 3. Four sets of peaks are seen, the central transition and the two satellite images arising from the SDS compartment, and the single image from the NaCl compartment. The two central images are shifted in opposite directions by the magnetic field gradient because the two compartments are separated along the z dimension (as shown in the schematic in Fig. 3A). The QFN sequence was used throughout, and only the pulse duration of the soft pulse was varied between 50 and 450 μs to show the approach of the optimal suppression condition for the free sodium signal. Along with the

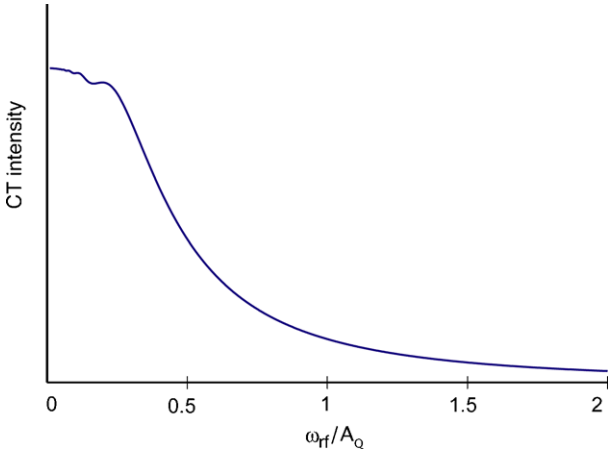

Fig. 2. Central transition intensity obtained in the QFN sequence as a function of the ratio $\frac{\omega_{rf}}{A_Q}$ for the soft pulse.

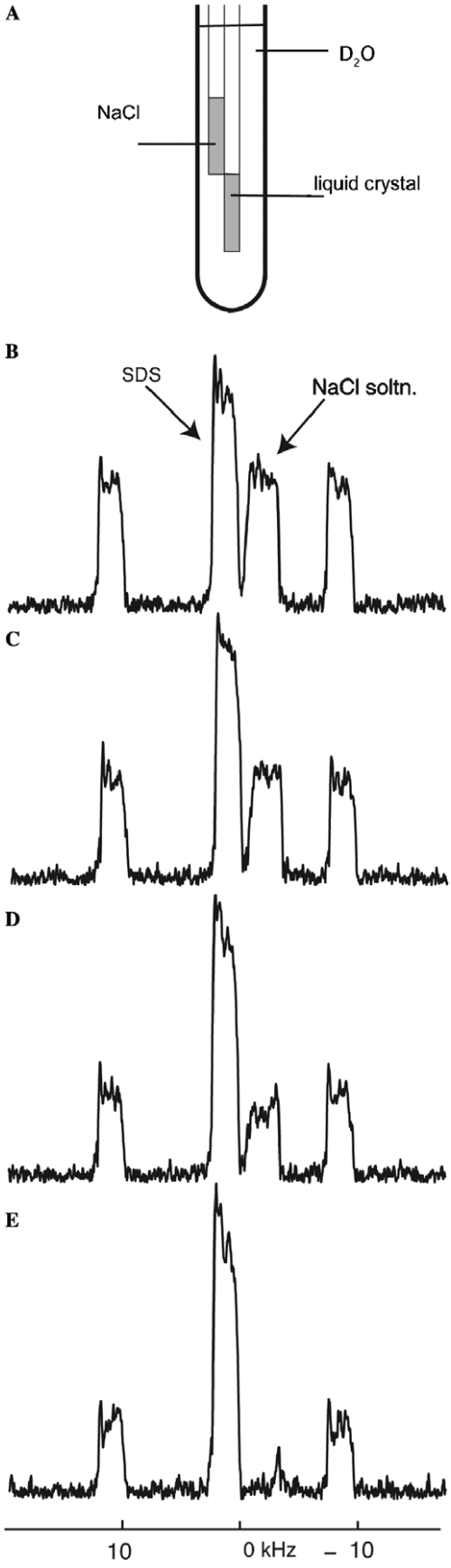

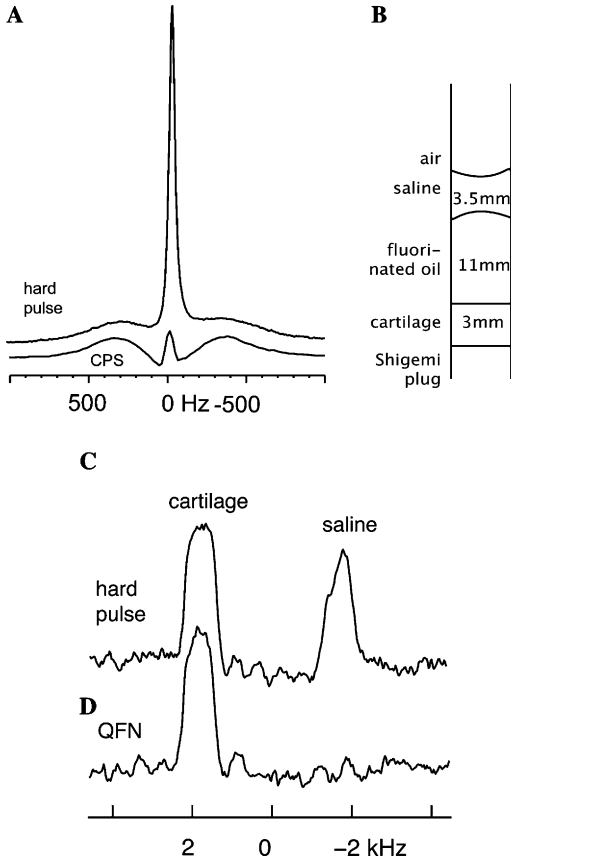

Fig. 4. (A) Cartilage/saline sample. (B) Hard pulse gradient spin echo experiment, both cartilage sodium and saline sodium are visible. (C) QFN experiment. The saline signals are suppressed in this experiment.

decrease of the free sodium signal, the intensity of the ordered sodium peak increases in accordance with the approach to a perfect inversion of the central transition populations by the soft pulse. As shown in Fig. 3E, a very good suppression of the free sodium signal can be obtained.

Fig. 4A shows a comparison between a hard pulse spectrum and a CPS spectrum of the cartilage plug. The sample showed a quadrupolar splitting centered at approximately $A_Q = 375$ Hz. For the 1D images the sample shown in Fig. 4B was used. Fig. 4C shows a hard pulse gradient spin echo image and Fig. 4D shows the QFN image. A very clean suppression of the free sodium signal is achieved in this case, even though sizeable inhomogeneity effects may be expected at the phase boundaries (Shigemi plug–cartilage, cartilage–fluorinert, fluorinert–water, water–air).

Fig. 3. Liquid crystalline test system. (A) Schematic of the sample used in our study. Two capillaries containing a NaCl solution and a liquid crystalline environment are used to separate the two compartments along the z direction. (B–E) One-dimensional images obtained using the QFN sequence. (B) 50, (C) 200, (D) 300, and (E) 450 μs soft pulse duration. The signal of free sodium is optimally suppressed in (E).

5. Conclusions

We presented a simple method that, by taking advantage of the unique rotational properties of a quadrupolar spin system, allows for the selective detection of the central transition of the ordered sodium signal from a sample containing sodium in both free and ordered environments. Its particular appeal lies in its simplicity: only two pulses are needed for it to work. Furthermore, we demonstrate the feasibility of the method in cartilage samples, where T_1 and T_2 are notoriously short. One could also use this trick to suppress the signal of ordered sodium, in which case it is sufficient to use a single pulse. The simplicity of setup makes this technique particularly easy to implement into existing imaging protocols. We also show that the method is not restricted to very small ratios of $\frac{\omega_{rf}}{A_Q}$. Furthermore, one could consider using sequences, in which the free sodium signal is rotated by angles larger than $\frac{\pi}{2}$, in which case the ordered sodium signal may be rotated to angles such as $\frac{3\pi}{2}$, and effective filtering may be achieved for larger ratios of $\frac{\omega_{rf}}{A_Q}$. Similar methods may be used for nuclei with spins larger than 3/2, where the ratios that can be employed will be even larger.

References

[1] S. Kohler, N. Kolodny, Sodium magnetic resonance imaging and chemical shift imaging, Prog. Nucl. Magn. Reson. Spectrosc. 24 (1992) 411–433.

[2] E. Shapiro, A. Borthakur, A. Gougoutas, R. Reddy, Na-23 MRI accurately measures fixed charge density in articular cartilage, Magn. Reson. Med. 47 (2002) 284–291.

[3] A. Borthakur, E. Shapiro, J. Beers, S. Kudchodkar, J. Kneeland, R. Reddy, Sensitivity of MRI to proteoglycan depletion in cartilage: comparison of sodium and proton MRI, Osteoarthritis Cartilage 8 (2000) 288–293.

[4] A. Wheaton, A. Borthakur, G. Dodge, B. Kneeland, H. Schumacher, R. Reddy, Sodium magnetic resonance imaging of proteoglycan depletion in an in vivo model of osteoarthritis, Acad. Radiol. 11 (2004) 21–28.

[5] A. Wheaton, A. Borthakur, E. Shapiro, R. Regatte, S. Akella, J. Kneeland, R. Reddy, Proteoglycan loss in human knee cartilage: quantitation with sodium MR imaging—feasibility study, Radiology 231 (2004) 900–905.

[6] A. Borthakur, E. Shapiro, S. Akella, A. Gougoutas, J. Kneeland, R. Reddy, Quantifying sodium in the human wrist in vivo by using MR imaging, Radiology 224 (2002) 598–602.

[7] E. Insko, D. Clayton, M. Elliott, In vivo sodium MR imaging of the intervertebral disk at 4 T, Acad. Radiol. 9 (2002) 800–804.

[8] R. Reddy, E. Insko, E. Noyszewski, R. Dandora, J. Kneeland, J. Leigh, Sodium MRI of human articular cartilage in vivo, Magn. Reson. Med. 39 (1998) 697–701.

[9] R. Kemp-Harper, S. Brown, C. Hughes, P. Styles, S. Wimperis, ^{23}Na NMR methods for selective observation of sodium ions in ordered environments, Prog. Nucl. Magn. Reson. Spectrosc. 30 (1997) 157–181.

[10] G. Navon, H. Shinar, U. Eliav, Y. Seo, Multiquantum filters and order in tissues, NMR Biomed. 14 (2001) 112–132.

[11] G. Jaccard, S. Wimperis, G. Bodenhausen, Multiple-quantum spectroscopy of $S = 3/2$ spins in isotropic phase: a new probe for multiexponential relaxation, J. Chem. Phys. 85 (1986) 6282–6293.

[12] U. Eliav, K. Keinan-Adamsky, G. Navon, A new method for suppressing the central transition in $I = 3/2$ NMR spectra with a demonstration for Na-23 in bovine articular cartilage, J. Magn. Reson. 165 (2003) 276–281.

[13] W. Ling, A. Jerschow, Selecting ordered environments in NMR of Spin-3/2 nuclei via frequency-sweep pulses, J. Magn. Reson. 176 (2005) 234–238.

[14] W. Ling, A. Jerschow, Frequency-selective quadrupolar MRI contrast, Solid-State Nucl. Magn. Reson. Spectrosc. 29 (2006) 227–231.

[15] A. Jerschow, From nuclear structure to the quadrupolar NMR Hamiltonian and high-resolution spectroscopy, Prog. Nucl. Magn. Reson. Spectrosc. 46 (2005) 63–78.

[16] S. Vega, Fictitious spin 1/2 operator formalism for multiple quantum NMR, J. Chem. Phys. 68 (1978) 5518–5527.

[17] A.P.M. Kentgens, Off-resonance nutation nuclear magnetic resonance spectroscopy of half-integer quadrupolar nuclei, Prog. Nucl. Magn. Reson. Spectrosc. 32 (1998) 141–164.

[18] MATLAB 7 for Macintosh. The MathWorks, Natick, MA, 2004.